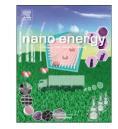Available online at www.sciencedirect.com

ScienceDirect

journal homepage: www.elsevier.com/locate/nanoenergy

RAPID COMMUNICATION

Binder-free three-dimensional silicon/carbon nanowire networks for high performance lithium-ion battery anodes

CrossMark

Wei Wang[a], Miao Tian[a], Yujie Wei[b], Se-Hee Lee[a],
Yung-Cheng Lee[a], Ronggui Yang[a],*

[a]Department of Mechanical Engineering, University of Colorado, Boulder, CO 80309, USA
[b]State Key Laboratory of Nonlinear Mechanics, Institute of Mechanics, Chinese Academy of Sciences, Beijing 100190, PR China

Abstract

The three-dimensional (3-D) nano-architectures have attracted tremendous attention for applications in lithium-ion (Li-ion) batteries due to their unique structural advantages. In this work, we developed a facile approach to fabricate 3-D Silicon (Si) nanowire networks. By precipitation, Si nanowires spontaneously interwove with one another to form 3-D nanowire networks with large amount of micro/nano gaps, which can not only facilitate Li-ion transport but also effectively accommodate the volume change. Carbon coating was then applied on Si nanowire networks through a chemical vapor deposition (CVD) process, which not only mechanically strengthens the structure but also helps the formation of 3-D electrical conducting network. A Si/C nanowire network with a wire diameter of 75 nm and 12 wt% of carbon coating exhibits a very high specific capacity of 2300 mAh g^{-1} at a rate of C/5 and a high specific capacity of around 600 mAh g^{-1} at a high rate of 4.5C. Our experimental investigations showed that the cycle life of such Si/C nanowire network can be further prolonged by increasing the carbon coating content, decreasing the diameters of Si nanowires, or reducing the testing voltage window. A Si/C nanowire network with a wire diameter of 37 nm and 17 wt% carbon coating can retain 78% of the initial capacity after 60 cycles in a testing voltage window of 0.1–2 V.
© 2013 Elsevier Ltd. All rights reserved.

Introduction

There are great demands for high-capacity and high-power lithium-ion (Li-ion) batteries for both portable electronics and electrical vehicles [1,2]. One of the key issues is to

*Corresponding author. Tel.: +1 303 735 1003; fax: +1 303 492 3498.
E-mail address: ronggui.yang@colorado.edu (R. Yang).

develop innovative battery materials and electrode structures [3]. Silicon (Si) has been broadly suggested to be a promising anode material for the next generation Li-ion batteries because of its highest theoretical capacity (>3500 mAh g^{-1}), which is around 10 times higher than that of the commercial graphite anodes (372 mAh g^{-1}) [4,5]. However, the ~300% volume expansion in most Si-based electrodes during the charge/discharge process leads to their limited cycle life [6]. Micro/nanostructured Si electrodes has thus gained increasing attention due to the possibility in volume change accomodation [6,7]. A capacity of >3500 mAh g^{-1}has been demonstrated in Si nanowire arrays [6]. Many different approaches have then been taken to improve the performance of one-dimensional Si nanostructures, such as Si nanotubes, c-Si/α-Si and C/Si core-shell nanowires [8-11]. However, the straight Si nanowire arrays are of unsatisfactory areal capacity with low mass loading density [8], where high-aspect ratio nanowire arrays would exhibit rapid performance degradation due to agglomeration and clustering of nanowires [12,13].

On the other hand, three-dimensional (3-D) self-supported network structure could potentially eliminate the agglomeration problem, and hence improve the structural stability and the battery performance due to the interconnected electron transport network and the native gaps for lithium ion diffusion [12-14]. Benefiting from the 3-D network structure, ultra-fast battery with a charge/discharge rate of over 1000 C was reported on a 3-D Ni/Li-Mn-O bicontinuous network[15], and significant enhancement of areal capacity and rate capability were also realized in 3-D Ni/TiO$_2$ and Ni-Sn nanowire networks using porous anodized alumina (PAA) templated synthesis method [12,13]. Better rate capabilities and cycle lives have also been demonstrated in silicon nanostructures including 3-D interconnected Si nanowires, inverse-opal Si and Ni/Si networks synthesized using silica sphere template-assisted chemical vapor deposition (CVD) or a modified CVD process [16-19].

In this work, we developed a facile and versatile process to fabricate the 3-D Si/C nanowire network using the *ex-situ* grown Si nanowires as building blocks, as shown in Fig. 1. The dispersed Si nanowires will entangle with each other during the precipitation process, and spontaneously interweave a 3-D nanowire network. On the basis of this unique structure, the kinetics process in Li-ion batteries can be potentially promoted, and consequently high capacity and the high-rate performance can be expected.

Material and methods

Preparation of Si/C nanowire network electrodes

Si nanowires with average diameters of 75 nm and 37 nm were fabricated through metal-assisted wet-etching method using

in-situ PAA templates as masks, where the details can be found in Ref. [20] and summarized in supporting information Section 1. As shown in Fig. 1, to fabricate the Si/C nanowire networks, 25 mg of Si nanowires were dispersed in 25 ml ethanol solution by ultrasonicating for 10 min and then transferred into a box. After evaporating the ethanol solution in ambient environment for 5 h, Si nanowires interwove with each other during the precipitation process and spontaneously formed a 3-D nano wire network. This nanowire precipitation process is rather universal and can be applied to abundant Si nanowires made through other processes [21-26]. The Si nanowire network was then coated with different thicknesses of carbon by decomposing ethylene through the CVD process for different durations of 2, 4, and 8 h at 700 °C. To study the electrochemical properties of the as-obtained Si/C nanowire networks, the electrodes for test were prepared by evaporating a 200 nm thick Cu film on the top of the Si/C nanowire network as the current collector. The gravimetric capacities presented in this paper were calculated based on the weight of the whole electrode including the Si nanowires, the carbon coating, and the evaporated Cu current collector layer.

Structural characterizations

The field-emission scanning electron microscopy (FE-SEM, JEOL JSM-7401F) equipped with the energy dispersive spectroscopy (EDS) was employed to examine the morphologies and composition of the as-prepared nanowire networks, and the microstructure of dispersed nanowires was studied using a transmission electron microscopy (TEM, Philips CM-10) and high resolution TEM (HRTEM, JEOL 2000 FX). The focused ion beam (FIB, FEI NOVA 660i) instrument was employed to cut the sample for cross-sectional morphology observation.

The detailed structural and compositional parameters of different Si/C nanowire network electrodes tested in this study are listed in Table 1. The Si nanowire diameter and the thickness of carbon coating are measured using HRTEM images. To accurately measure the mass loading of the pure Si nanowire network, the mass (M) of every sample with a size of 3.5×6.5 cm^2 had been weighed. The mass loading (ρ_A) of pure Si nanowire network can be calculated as $\rho_A=M/(3.5\times6.5)$ mg cm^{-2}. The Cu layer content can be calculated by weighting the sample before and after evaporating the 200 nm Cu film. The carbon content of the electrode was then calculated by weighting the Si/C nanowire networks before and after heating the sample in ambient environment at 600 °C for 1 h, where the carbon can be burnt thoroughly and the color of sample changed from black to the original yellow color of the pure Si nanowire network [27]. There is negligible mass increase due to the oxidization of Si nanowires as we observed less than 0.5% weight difference in a reference pure
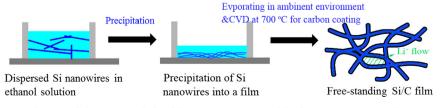

Fig. 1 Schematics of the fabrication process of Si/C nanowire network.

Si nanowire network going through the same heating/burning process.

Electrochemical measurements

The free-standing Si/C nanowire network electrodes were then punched into a 7/16 in. diameter disk and assembled into CR2032 coin cells with Li metal as counter electrodes and 1 M LiPF$_6$ in ethylene carbonate (EC)/dimethyl carbonate (DMC) (1:1 volume ratio, Aldrich) as the electrolyte in an argon-filled glove box. Due to the intrinsic interconnections in the 3-D network structure, no binder material is used in this Si/C nanowire network electrode. The Si/C nanowire network using Si nanowires with the diameter of 75 nm is named as the "75 nm Si/C nanowire network" for short, and the one using Si nanowires with diameter of 37 nm is denoted

as the "37 nm Si/C nanowire network". As a comparison, we also fabricated "milled 75 nm Si/C nanowire electrode" using a process similar to the traditional electrode preparation process (See Supporting Information Section 2) [7]. The electrochemical performance was tested with a computer controlled battery testers (MTI, 5V1mA and 5V5mA) within the voltage windows of 0.01–2 V and 0.1–2 V.

Results and discussion

Fig. 2a shows the optical image of one piece of 9×9 cm^2 Si nanowire network consisting of Si nanowires with an average diameter of 75 nm. Figs. 2b and c show the top-view SEM image of the 75 nm Si nanowire network without and with CVD carbon coating. In both images, Si nanowires interweave with one another, with spontaneously formed micro/nano gaps at a

Table 1 Structural and compositional parameters of the tested Si/C nanowire network electrodes consisted of Si nanowire network, carbon coating, and evaporated Cu layer.

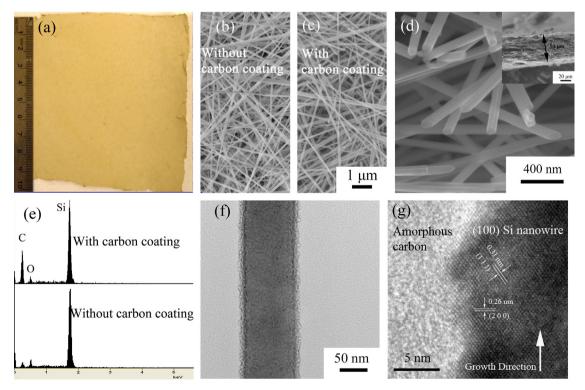| #	Si nanowire diameters (nm)	CVD time (h)	Carbon coating thickness (nm)	Carbon content (%)	Cu layer content (%)	Areal density (mg.cm^{-2})	Volumetric density (g.cm^{-3})
1	75	2	~3	4	8	1.34	~0.27
2	75	4	~6	8	7	1.46	~0.29
3	75	8	~10	12	7	1.52	~0.3
4	37	8	~10	17	6	1.82	~0.55

Fig. 2 (a) Optical image and (b) top-view FE-SEM image of a free-standing 75 nm Si nanowire network without carbon coating; (c) top-view FE-SEM image of the 75 nm Si/C nanowire network with 12 wt% carbon (the scale bar is same for both of (b) and (c)); (d) cross-sectional FE-SEM images of 75 nm Si/C nanowire network with 12 wt% carbon after FIB milling process, the inset is the cross-sectional image of the 75 nm Si/C nanowire network; (e) EDS results of the 75 nm Si nanowire network without and with carbon coating, (f) TEM image of one individual 75 nm Si/C core–shell nanowire and (g) HRTEM image of the Si–C interface.

size range of tens of nanometers to a few micrometers. Fig. 2d shows the cross-sectional FE-SEM image of the 75 nm Si/C nanowire network with 8-h CVD carbon coating after FIB milling process. Apparently the nanoscale gaps are retained after the CVD coating process. The inset of Fig. 2d shows that the sample thickness of the as-obtained Si/C nanowire network is about 50 μm. The EDS results in Fig. 2e shows an increased carbon signal after 8-h CVD carbon coating. An individual Si/C nanowire was characterized by the TEM after dispersing the sample in ethanol with ultrasonication for 20 min. Fig. 2f shows a conformal carbon coating layer with a thickness of about 10 nm along the single Si nanowire. The silicon nanowire surface roughness originates from the wet etching process [28]. The HRTEM image in Fig. 2g indicates that the Si nanowires is single crystalline and the carbon coating is amorphous. The fringe spacings show good agreement with the lattice spacings of (2 0 0) and (1 1 1) planes as a cubic Si phase (JCPDS 80-0018), respectively. The result confirms that the [1 0 0] crystal orientation of the Si nanowires is the same as the original Si wafer orientation [29].

Fig. 3a compares the gravimetric discharge (lithiation) capacity of the 75 nm Si nanowire network without carbon coating, the Si/C nanowire network with 75 nm diameter Si nanowires and 12 wt% carbon coating, and the milled 75 nm Si/C nanowire electrode. The 75 nm Si/C nanowire network and the milled 75 nm Si/C nanowire electrodes were tested at a current density of $0.4 \, A \, g^{-1}$ in the testing voltage window of 0.01–2 V, while the Si nanowire network without carbon coating was tested at a lower current density of $0.12 \, A \, g^{-1}$ since it exhibited a negligible capacity at the current density of $0.4 \, A \, g^{-1}$ (see Supporting Information Section 3). A discharge capacity of $1800 \, mAh \, g^{-1}$ at the first cycle was observed for the 75 nm Si nanowire network without carbon coating, which, however, drops dramatically to almost zero in 6 cycles. The 75 nm Si/C nanowire network with 12 wt% carbon exhibits a higher discharge capacity of $2600 \, mAh \, g^{-1}$ at the first cycle, and, more importantly, a much better cycling stability. The discharge capacity is 2000–$2300 \, mAh \, g^{-1}$ at the rate of $C/5$ in the next 20 cycles when a current of $0.4 \, A \, g^{-1}$ is applied (C/n is referred as the charge/discharge rate to complete one charge/discharge cycle with full capacity C in n hours). The improvement in the 3-D Si/C nanowire network is attributed to the carbon coating, which has been widely used in various cathode and anode materials to improve the electrical conductivity and to provide the surface protection [18,30]. Besides that, the carbon coating in this 3-D Si nanowire network serves as the bonding layer to enhance the mechanical rigidity of the Si nanowire electrode. Fig. 3b shows the stress-strain behavior of the Si nanowire network with and without carbon coating. For each kind of samples, three specimens have been tested. The detailed experimental procedure is presented in the Supporting Information Section 4. The 75 nm Si nanowire networks without carbon coating were broken at failure strength of about 0.5 MPa. In contrast, the strength of the Si/C nanowire network was greatly enhanced and it reaches 5 MPa, which was 10 times higher than that of the Si nanowire networks without carbon coating. In the pure Si nanowire network, the Si nanowires are simply next to each other without any intrinsic connection between the neighboring nanowires. After carbon coating, the carbon will wrap the nanowires and leads to the formation of interconnection between the Si

nanowires. Thus, the mechanical strength can be greatly enhanced. The great enhancement of mechanical strength in 75 nm Si/C nanowire network with 12 wt% carbon suggests that the carbon coating could effectively strengthen the connections between Si nanowires in the network, and give rise to better mechanical stability of the electrode during electrochemical cycling.

On the other hand, a discharge capacity of $2200 \, mAh \, g^{-1}$ was delivered by the milled 75 nm Si/C nanowire electrode during the first cycle. However, it quickly drops to almost zero within 14 cycles. To understand the failure mechanism on the milled sample, the corresponding morphology was examined by FE-SEM, which indicates that the Si/C nanowires had been broken into short nanorods during the milling and mixing process (see Supporting Information Section 2). The connection between the Si nanowires was seriously destroyed although the silicon nanowire surfaces have been coated with CVD carbon. The PVDF binder materials and AB carbon are not able to maintain the stable
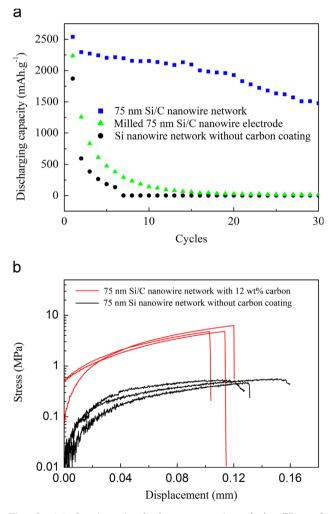

Fig. 3 (a) Gravimetric discharge capacity of the 75 nm Si nanowire networks without carbon coating, the milled 75 nm Si/C nanowire electrode and the 75 nm Si/C nanowire network with 12 wt% carbon, tested at $0.4 \, A \, g^{-1}$; and (b) stress-displacement relations of the 75 nm Si nanowire network without carbon coating and the 75 nm Si/C nanowire network with 12 wt% carbon.

electrical connection among Si nanostructures [31]. The lack of continuous electron transport pathways in the milled Si/C nanowire electrode would unavoidably lead to capacity degradation.

We had also systematically studied the effect of carbon coating content on the galvanostatic cycling performance of the Si/C nanowire networks. As shown in Fig. 4a, all the 75 nm Si/C nanowire network samples with carbon content of 4 wt%, 8 wt% and 12 wt% after CVD carbon coating processes for 2, 4 and 8 h exhibit high discharge capacity of over 2000 mAh g^{-1} for more than 10 cycles. The Coulombic efficiencies of these Si/C nanowire networks at the first cycle are as high as 91% compared to the 60-80% in most other Si based electrodes [7,32,33], and the Coulombic efficiencies increases to beyond 98% in later cycles. However, the discharge capacity degrades during cycling and drops in a faster rate after 10-20 cycles. There is an obvious transition point of the capacity degradation rate as the slope changes in all three curves. When the carbon content is increased from 4 wt% to 12 wt%, the transition point of the capacity degradation rate is delayed
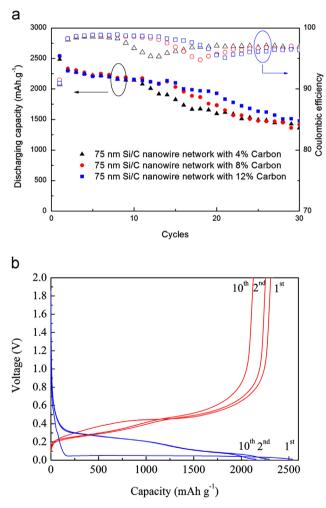

from the 13th to the 21st cycle. This indicates that thicker carbon coating can provide a more stable structure for better cycling performance. Fig. 4b shows the galvanostatic discharge/charge curves of the 75 nm Si/C nanowire network with 12 wt% carbon. It shows a large irreversible discharge capacity at the first cycle with a plateau at around 0.05 V, which is consistent with other results of single crystalline Si [10,34]. The large irreversible capacity at the first cycle is due to the irreversible transition from crystalline Si to amorphous Li$_x$Si and also the formation of SEI layer [33,35]. After the second cycle, it exhibits the typical electrochemical behavior of Li$_x$Si with a flat reversible discharge voltage plateau in the range of 0.2-0.6 V and a charge voltage plateau in the range of 0.01-0.4 V [10,36].

Fig. 5 shows that the anode performance of the Si/C nanowire networks can be improved by reducing the diameters of Si nanowires and the testing voltage windows. All the tested samples were CVD-coated with carbon for 8 h. When the nanowire diameter decreases from 75 nm to 37 nm, the discharge capacity decreases slightly to around 1700 mAh g^{-1} which might be due to the higher weight percentage of carbon (17 wt% comparing to 12 wt%) and a little higher C-rate (C/4 comparing to C/6). However, the stability is improved greatly in 37 nm Si/C nanowire network with 17 wt% carbon. The transition point of discharge capacity degradation rate changes to the 30th cycle compared to the 21st cycle in 75 nm Si/C nanowire network with 12 wt% carbon. On the other hand, the structural stability can also be improved by reducing the testing voltage window which reduces the amount of Li ions inserted. Due to the low initial discharge plateau at about 0.03-0.05 V shown in Fig. 4b, Si/C nanowire networks were tested in the voltage window of 0.01-2 V for the first cycle to activate the lithiation of crystalline Si nanowires. The testing voltage window was changed after the first cycle to 0.1-2 V. Starting from the fifth cycle, the discharge capacity turns to be stable around 1200 mAh g^{-1} for 75 nm Si/C nanowire network with 12 wt% carbon and around 1000 mAh g^{-1} for the 37 nm Si/C nanowire network with 17 wt% carbon. Meanwhile, the cycle life is greatly improved by reducing the voltage window. Fig. 5b presents the discharge capacity normalized by the discharge capacity at the fifth cycle. The 37 nm Si/C nanowire network with 17 wt% carbon retains 78% of the initial capacity over 60 cycles in the voltage window of 0.1-2 V compared to 40% in the voltage window of 0.01-2 V.

Fig. 6 shows the rate capability of Si/C nanowire network anodes with Si nanowire diameters of 75 nm and 37 nm, both with 8-h CVD carbon coating and tested in the charge/discharge testing window of 0.01-2 V. For both of samples tested, the testing current density was doubled every four cycles with the initial current density of 0.2 A g^{-1}. At the low current density of 0.2 A g^{-1}, the discharge capacity can reach 2500 mAh g^{-1} for the 75 nm Si/C nanowire network and 1800 mAh g^{-1} for the 37 nm Si/C nanowire network. While the current density is increased to be 3.2 A g^{-1}, the discharge capacity remains 25% of the initial discharge capacity for both of the samples, as shown in the inset of Fig. 6. It is worthwhile to mention that a high discharge capacity of 600 mAh g^{-1} at a high rate of 4.5C is observed for the 75 nm Si/C nanowire network with 12 wt% carbon, which is larger than the theoretical capacity of commercial graphite (372 mAh g^{-1}) and 5 times higher than that of annealed graphite at the

Fig. 4 (a) Gravimetric discharge capacity of 75 nm Si/C nanowire network with different carbon coatings tested at 0.4 A g^{-1} and the corresponding Coulombic efficiencies (to the right axis), and (b) galvanostatic discharge/charge curves of 75 nm Si/C nanowire network with 12 wt% carbon tested at 0.4 A g^{-1}.
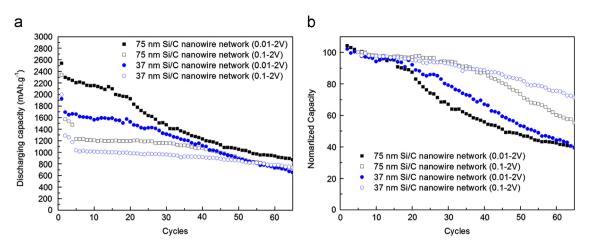
Fig. 5 (a) Gravimetric discharge capacity and (b) normalized discharge capacity, of 75 nm Si/C nanowire network with 12 wt% carbon and 37 nm Si/C nanowire network with 17 wt% carbon tested at different testing voltage windows.
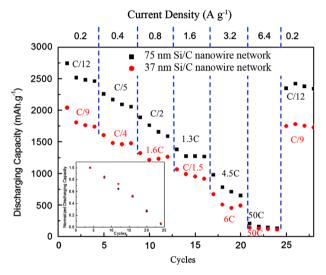

Fig. 6 Rate capabilities of the 75 nm Si/C nanowire network electrode with 12 wt% carbon (black square) and the 37 nm Si/C nanowire network electrode with 17 wt% carbon (red circle); the discharge capacity of last cycle in every four cycle is normalized by the discharge capacity at the fourth cycle, and the inset is the normalized capacities *vs.* cycles. (For interpretation of the references to color in this figure legend, the reader is referred to the web version of this article.)

same rate [37]. It is a little higher than that of the 3-D inverse-opal Si networks and comparable to that of the 3-D Ni/Si bicontinuous networks based on 500 nm colloid template, which both form 3-D porous electrodes for Li-ion penetration [18,19]. One would expect a better rate capability for the smaller nanowires with shorter Li ion diffusion length. However, the rate capabilities for Si/C nanowire network with diameters of both 75 nm and 37 nm are quite close to each other, as shown in inset of Fig. 6, which is likely due to the density difference of the samples. As seen in Table 1, the volumetric density of the 37 nm Si/C nanowire network with 17 wt% is 0.55 g cm^{-3}, which is much higher than that of the 75 nm Si/C nanowire network with 12 wt% carbon, ~0.3 g cm^{-3}. Higher density results in less empty space for both Li-ion flow and volume exchange accommodation [38].

To understand the failure mechanism of the Si/C nanowire network in Li-ion batteries, the 75 nm Si/C nanowire network with 12 wt% carbon after testing for 70 cycles with a testing current density of 0.4 A g^{-1} was cleaned with DMC solution in a glove box, and then examined by FE-SEM and TEM, as shown in Fig. 7a and b. The nanowires are significantly bended compared to the straight and smooth nanowires before cycling in Fig. 2b. Compared to the 75 nm dense Si nanowire with clear carbon coating in thickness of 10 nm on surface, the Si/C core–shell nanowire becomes porous with a expanded diameter of 140-150 nm. The morphgies are consistent with other reports because the huge volume expansion of >300% can lead to the structure expansion of 160% in the axial and radius directions, respectively [6,39]. Nanopores can be gradually genernated during the cycling process, which has been demonstrated in ZnO and Si nanowires [40]. Such volume expansion could result in the capacity degradation through two possible mechanisms: (1) it leads to the pulverization in Si nanowires [6]. However, as demonstrated in Fig. 7a, the Si nanowires continuous with a bended morphology and do not break into short nanorods or nanoparticles. Both of the theoretical and experimental works have demonstrated that the Si nanostructures with dimensions smaller than 150 nm are able to survive during the structure expansion [6,41,42]. (2)Very likely, it breaks the connection between active Si and conducting materials [43,44]. As schemed in Fig. 7c, the lithiation process results in the structure expansion both in radius direction and along the nanowire. The volume expansion in the radius direction will break the interconnection due to the large volume expansion mismatch between the active Si (>300%) and the conducting carbon layer (9%) [35]. The volume expansion along the nanowire would lead to the bending of nanowires and thus a stress is generated at the interface between Si nanowires. The repeating expanding and shrinking will make the interconnections loose. Once it reaches the fatigue strength of the carbon bonding layer, the Si nanowires will lose the connection to the electrode system, and cannot contribute to the capacity and thus results in the capacity degradation of electrode. Thus, the transition point of the capacity degradation rate appeared. It is consistent with our results that the pure Si nanowire network without carbon coating exhibits rapid capacity degradation, and the more carbon coating can provide stronger bonding strength and hence longer cycle life.
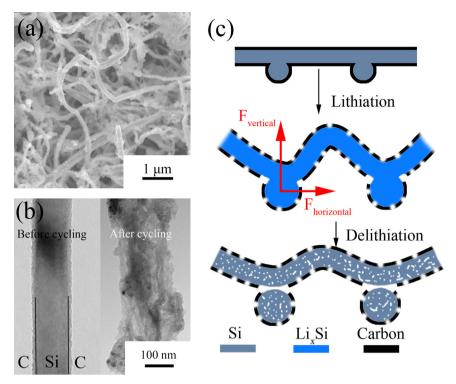
Fig. 7 (a) Top-view FE-SEM image of 75 nm Si/C nanowire network with 12 wt% carbon after testing for 70 cycles at a testing current of 0.4 A g^{-1}; (b) TEM image of Si/C nanowire before and after testing for 70 cycles; and (c) schematics of possible failure mechanism on the Si/C nanowire network.

Conclusions

We have successfully fabricated the 3-D Si/C nanowire networks by CVD carbon coating on facile-precipitated Si nanowire network. Si nanowires are connected to one another with spontaneous formation of micro/nano gaps, which is beneficial for Li-ion flow and volume expansion accommodation. In the 75 nm Si/C nanowire network with 12 wt% carbon, a very high discharge capacity of 2300 mAh g^{-1} at a rate of *C*/5 has been achieved, and a high capacity of about 600 mAh g^{-1} is reached at a very high discharge rate of 4.5*C*. The cycle life can be increased by increasing the carbon coating content with a stronger bonding strength, decreasing the diameters of Si nanowires, and reducing the testing voltage window to alleviate volume expansion.

Acknowledgment

Appendix A. Supporting information

Supplementary data associated with this article can be found in the online version at: http://dx.doi.org/10.1016/j.nanoen.2013.03.015.

References

[1] C. Liu, F. Li, L.P. Ma, H.M. Cheng, Advanced Materials 22 (2010) E28.
[2] R.F. Nelson, Journal of Power Sources 91 (2000) 2.
[3] M. Armand, J.-M. Tarascon, Nature 451 (2008) 652.
[4] Y. He, X.Q. Yu, Y.H. Wang, H. Li, X.J. Huang, Advanced Materials 23 (2011) 4938.
[5] U. Kasavajjula, C.S. Wang, A.J. Appleby, Journal of Power Sources 163 (2007) 1003.
[6] C.K. Chan, H.L. Peng, G. Liu, K. McIlwrath, X.F. Zhang, R.A. Huggins, Y. Cui, Nature Nanotechnology 3 (2008) 31.
[7] H.J. Kim, M.H. Seo, M.H. Park, J.P. Cho, Angewandte Chemie International Edition 49 (2010) 2146.
[8] C.K. Chan, R.N. Patel, M.J. O'Connell, B.A. Korgel, Y. Cui, ACS Nano 3 (2010) 1443.
[9] M.H. Park, M.G. Kim, J. Joo, K. Kim, J. Kim, S. Ahn, Y. Cui, J. Cho, Nano Letters 9 (2009) 3844.
[10] L.F. Cui, R. Ruffo, C.K. Chan, H.L. Peng, Y. Cui, Nano Letters 9 (2009) 491.
[11] L.F. Cui, Y. Yang, C.M. Hsu, Y. Cui, Nano Letters 9 (2009) 3370.
[12] M. Tian, W. Wang, Y.J. Wei, R.G. Yang, Journal of Power Sources 211 (2012) 46.
[13] W. Wang, M. Tian, A. Abdulagatov, S.M. George, Y.-C. Lee, R.G. Yang, Nano Letters 12 (2011) 655.

[14] M. Rauber, I. Alber, S. Müller, R. Neumann, O. Picht, C. Roth, A. Schokel, M.E. Toimil-Molares, W. Ensinger, Nano Letters 11 (2011) 2304.

[15] H.G. Zhang, X.D. Yu, P.V. Braun, Nature Nanotechnology 6 (2011) 277.

[16] H.T. Nguyen, F. Yao, M.R. Zamfir, C. Biswas, K.P. So, Y.H. Lee, S.M. Kim, S.N. Cha, J.M. Kim, D. Pribat, Advanced Energy Materials 1 (2011) 1154.

[17] Y. Yao, M.T. McDowell, I. Ryu, H. Wu, N. Liu, L.B. Hu, W.D. Nix, Y. Cui, Nano Letters 11 (2011) 2949.

[18] A. Esmanski, G.A. Ozin, Advanced Functional Materials 19 (2009) 1999.

[19] H.G. Zhang, P.V. Braun, Nano Letters 12 (2012) 2778.

[20] W. Wang, D. Li, M. Tian, Y.C. Lee, R.G. Yang, Applied Surface Science 258 (2012) 8649.

[21] M.S. Gudiksen, C.M. Lieber, Journal of the American Chemical Society 122 (2000) 8801.

[22] D.P. Yu, Z.G. Bai, Y. Ding, Q.L. Hang, H.Z. Zhang, J.J. Wang, Y.H. Zou, W. Qian, G.C. Xiong, H.T. Zhou, S.Q. Feng, Applied Physics Letters 72 (1998) 3458.

[23] J. Mallet, M. Molinari, F. Martineau, F. Delavoie, P. Fricoteaux, M. Troyon, Nano Letters 8 (2008) 3468.

[24] Z.P. Huang, N. Geyer, P. Werner, J. de Boor, U. Gösele, Advanced Materials 23 (2011) 285.

[25] C. Chiappini, X.W. Liu, J.R. Fakhoury, M. Ferrari, Advanced Functional Materials 20 (2010) 2231.

[26] M.L. Zhang, K.Q. Peng, X. Fan, J.S. Jie, R.Q. Zhang, S.T. Lee, N.B. Wong, The Journal of Physical Chemistry C 112 (2008) 4444.

[27] H. Wu, G. Chan, J.W. Choi, I. Ryu, Y. Yao, M.T. McDowell, S.W. Lee, A. Jackson, Y. Yang, L.B. Wu, Y. Cui, Nature Nanotechnology 7 (2012) 309.

[28] A.I. Hochbaum, R.K. Chen, R.D. Delgado, W.J. Liang, E.C. Garnett, M. Najarian, A. Majumdar, P.D. Yang, Nature 451 (2008) 163.

[29] K.Q. Peng, Y.J. Yan, S.P. Gao, J. Zhu, Advanced Materials 14 (2002) 1164.

[30] Y. Zhang, Q.Y. Huo, P.P. Du, L.Z. Wang, A.Q. Zhang, Y.H. Song, Y. Lv, G.Y. Li, Synthetic Metals 162 (2012) 1315.

[31] I. Kovalenko, B. Zdyrko, A. Magasinski, B. Hertzberg, Z. Milicev, R. Burtovyy, I. Luzinov, G. Yushin, Science 334 (2011) 75.

[32] P.F. Gao, H.P. Jia, J. Yang, Y.N. Nuli, J.L. Wang, J. Chen, Physical Chemistry Chemical Physics 13 (2011) 20108.

[33] X.J. Feng, J. Yang, P.F. Gao, J.L. Wang, Y.N. Nuli, RSC Advances 2 (2012) 5701.

[34] M.N. Obrovac, L.J. Krause, Journal of the Electrochemical Society 154 (2007) A103.

[35] S.C. Zhang, Z.J. Du, R.X. Lin, T. Jiang, G.R. Liu, X.M. Wu, D.S. Weng, Advanced Materials 22 (2010) 5378.

[36] L.F. Cui, L.B. Hu, J.W. Choi, Y. Cui, ACS Nano 4 (2010) 3671.

[37] A. Magasinski, P. Dixon, B. Hertzberg, A. Kvit, J. Ayala, G. Yushin, Nature Materials 9 (2010) 353.

[38] W. Lai, C.K. Erdonmez, T.F. Marinis, C.K. Bjune, N.J. Dudney, F. Xu, R. Wartena, Y.M. Chiang, Advanced Materials 22 (2010) E139.

[39] X.H. Liu, L.Q. Zhang, L. Zhong, Y. Liu, H. Zheng, J.W. Wang, J.H. Cho, S.A. Dayeh, S.T. Picraux, J.P. Sullivan, S.X. Mao, Z.Z. Ye, J.Y. Huang, Nano Letters 11 (2011) 2251-2258.

[40] J.W. Choi, J. McDonough, S. Jeong, J.S. Yoo, C.K. Chan, Y. Cui, Nano Letters 10 (2010) 1409-1413.

[41] X.H. Liu, L. Zhong, S. huang, S.X. Mao, T. Zhu, J.Y. Huang, ACS Nano 2 (2012) 1522-1531.

[42] S. Golmon, K. Maute, S.H. Lee, M.L. Dunn, Applied Physics Letters 97 (2010) 033111.

[43] C.J. Yu, X. Li, T. Ma, J.P. Rong, R.J. Zhang, J. Shaffer, Y.H. An, Q. Liu, B.Q. Wei, H.Q. Jiang, Advanced Energy Materials 2 (2012) 68-73.

[44] J.P. Maranchi, A.F. Hepp, A.G. Evans, N.T. Nuhfer, P.N. Kumta, Journal of the Electrochemical Society 153 (2006) A1246-A1253.
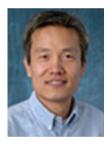
Wei Wang received his BS in Materials Physics (2003) and PhD in Condensed Matter Physics (2008) from University of Science and Technology of China, and he is a post-doctor in Department of Mechanical Engineering at University of Colorado - Boulder. His current research focuses on micro/nano-manufacturing of three-dimensional architectures for energy harvesting and storage applications.

Miao Tian is now a graduate student in Departmert of Mechanical Engineering at University of Colorado - Boulder. She received her BS degree from Xi'an Jiaotong University in 2007. Her current research foucuses on fabrication of three-dimensional nanostructures for Lithium-ion battery applications.

Yujie Wei is now a Professor at Institute of Mechanics, Chinese Academy of Sciences. He receiced his BS degree in Mechanics from Beijing University in 1997, and earned his PhD degree in Applied Mechanics from Massachusetts Institute of Technology in 2006. His research focuses on mechanics of materials.

Se-hee Lee is an Associate Professor in Department of Mechanical Engineering at University of Colorado - Boulder. He receiced his BS degree (1991) in Metallurgical Engineering and earned his PhD degree (1997) in Materials Science and Engineering from Seoul National University. His primary research interests have concentrated on nanostructured materials for energy applications.

Yung-Cheng (YC) Lee received his BSME degree from the National Taiwan University in 1978, and the M.S. and Ph.D. degrees from the University of Minnesota, in 1982 and 1984, respectively. Y. C. Lee is S.J. Archuleta Professor of Mechanical Engineering and the Director of DARPA Center on Nanoscale Science and Technology for Integrated Micro/Nano-Electromechanical Transducers (iMINT) at the University of Colorado-Boulder. Dr. Lee's research focuses on the integration of microelectromechanical systems (MEMS) and nanoelectromechanical systems (NEMS) with microelectronic, optoelectronic and microwave devices.

Ronggui Yang (Ph.D MIT 2006, MS MEMS-UCLA 2001, MS Thermophysics –Tsinghua 1999, BS Thermal Engineering-Xi'an Jiaotong Univ 1996) is an Assocaite Professor of Mechanical Engineering at the University of Colorado - Boulder. His research interests are on the fundamentals of nanoscale transport phenomena and the applications of micro/nanotechnologies for energy conversion, storage and thermal.